Capacity-Based Optimization Using Whale Optimization Technique of a Power Distribution Network

Bawoke Simachew[1], Baseem Khan[2], Josep M Guerrero[3], Sanjeevikumar Padmanaban[4], Om Prakash Mahela[5], Hassan Haes Alhelou[6]
[1]Department of Electrical Engineering, Wolaita Sodo University, Wolaita Sodo, Ethiopia
[2]Department of Electrical and Computer Engineering, Hawassa University, Ethiopia
[3]Center for Research on Microgrids – CROM, Aalborg University, Denmark
[4]Aalborg University, Denmark
[5]Power System Planning Division, Rajasthan Rajya Vidyut Prasaran Nigam Ltd., Jaipur, India
[6]Department of Electrical Power Engineering, Tishreen University, Lattakia, SY

**Corresponding Author: Baseem Khan, baseem.khan04@gmail.com*

Abstract-In the power distribution network, real power loss and voltage profile management are critical issues. By providing active and reactive power support, both of these issues can be managed. This paper utilized the Meta heuristic-based method for the optimal size and placement of distributed generation (DG) and capacitor (QG) sources for loss reduction by incorporating network current carrying capacity constraint in the optimization problem. The overall problem is optimized using an upgraded method of the fitness assignment and solution chasing based on the aggregate approach called Multi-objective Whale Optimization Algorithm (MWOA). Wind and solar photovoltaic sources are utilized as the distributed generation with their probabilistic outputs. The developed method is tested using two feeders of practical Bahir Dar Distribution Network, Ethiopia. The results of loss minimization and voltage profile management with MWOA are compared with multi-objective particle swam optimization (MPSO) with an equal number of iteration to show the superiority of the developed method.

Index Term: Whale Optimization Algorithm, Distributed Generation, Shunt capacitor placement, Particle Swarm Optimization, Loss minimization

1. Introduction

In distribution system, voltage is stepped down; as a result, system loss is higher. According to the Electric Power Research Institute (EPRI) [1, 2], the distribution loss is about 70 percent of all the energy loss and it is even higher during peak load conditions. It is indicated by various researchers that the distribution system has more than 13% losses of the total energy production. Therefore, the distribution loss minimization is the major issue in the smart grid system.

Various researchers utilized the meta-heuristic algorithms for the distribution system loss optimization. In [3], Ali et al. utilized mixed-integer linear programming optimization (MINLP) technique to size and place the battery-coupled distributed photovoltaic generators along with genetic algorithm (GA). In [4], Lalitha, et al. applied symbiotic organisms search (SOS) technique to find and locate the DG and QG optimally. In [5], Abdelaziz, et al. used flower pollination optimization (FPA) technique and power loss index for the capacitor optimal location and sizing and to reduce the overall cost and power loss. In [6], Reddy, et al. utilized WOA for the optimal sizing of renewable energy resources. In [7], Wang et al. used PSO for the reactive power optimization and sizing of the capacitor in radial distribution feeders. Bhulla et al. (2018) [8] used the artificial bee colony and cuckoo search hybrid technique for optimal integration of multi-distributed production. In [9], Xie et al. presented reactive power optimization for distribution network based on distributed random gradient-free algorithm. In [10], Boktor et al. proposed optimal distribution power flow including shunt capacitor allocation. In [11], Elsheikh et al. proposed optimal capacitor placement and sizing for radial electric power systems. In [12], Thang and Minh proposed optimal allocation and sizing of capacitors for distribution systems reinforcement. In [13], Hassanzadeh Farda et al. used PSO for sizing and placement of the renewable energy-based DG units in distribution systems by considering load growth. In [14], Prakash et al. proposed an optimal siting of capacitors in radial distribution system using WOA. In [15], Kumar et al. proposed an optimal placement and sizing of renewable distributed generations and capacitor banks for radial distribution networks. In [16], same authors developed multi-objective PSO based optimal placement of solar power distributed generation in radial distribution network.

This work mainly focused on the placement of the DG units but not focused on the reactive power support. None of above mentioned researchers considered:

1. Total feeders' carrying capacity as only limits to get the maximum possible active power loss
2. It is optimally quantifying and locating the DG and QG within the limit of assigned DG/QG size or choosing the arbitrary size of DG and QG out limits whenever there is a possible minimum power loss in the limit of network capacity (upper limit constraint).

Therefore, this study focused on the total real power loss reduction with voltage profile improvement of the two critical feeders in the Bahir Dar distribution network by optimally quantifying and locating the distributed generation (DG) and capacitors (QG) with the incorporation of the practical network or by choosing the arbitrary size of DG and QG if there is a possible minimum power loss in the limit of network capacity (upper limit constraint). For perform this research, a recent optimization technique called whale optimization algorithm [17] is utilized. Incorrect size of DG and QG may increase the system losses as compared to the base case condition. WOA is utilized for the proper site and size of the shunt capacitor and DG. Further, it is applied to locate and size of the capacitors. Therefore, in this work, multi-objective WOA (MWOA) is used for optimal sizing and siting of DG and QG. Further, this work utilized a mechanism called feeder carrying capacity limit as the constraint condition for the distribution network optimization. It is mentioned that DG and QG size must be less than the total power required by the system. Therefore, for the purpose of network security, in this work, 80% of the total power demand is taken as the upper limit of DG and QG.

The significant contributions of this work are as follows:

1. Two practical feeders of the Bahir Dar distribution network are considered and modelled to know the performance of the actual system
2. Multi-objective WOA is utilized to perform the optimal placement and sizing of the DG and QG sources in the system
3. Actual local metrological solar irradiation and wind speed data are considered to assess the energy outputs from the distributed generation sources
4. A detailed comparative analysis of the developed MWOA method is performed with MPSO which shows the superiority of the MWOA

The paper is organized as follows: section two discusses the description of the study area. Section three presents the selection and assessment of the active and reactive power generation resources. Section four presents the methodology and problem formulation. Section five presents the numerical results analysis and comparative analysis, followed by the conclusion.

2. Description of the Study Area

This work performed on the Ghion and Bata feeder of the Bahir Dar distribution network. Bahir Dar substation-II has the 230/132/15 kV and 230/66/15 kV buses, which are power sources to four feeders (i.e. Air force, Bata, Ghion and Papyrus) and the other substation-I supply three feeders (i.e. Sematate, Boiler and Industry). For this study, two feeders namely Ghion and Bata are selected, because the real power losses as well as the voltage violations at these feeders are beyond the permissible limits. Figure 1 and 2 presented the single line diagrams of Ghion and Bata feeders, respectively.

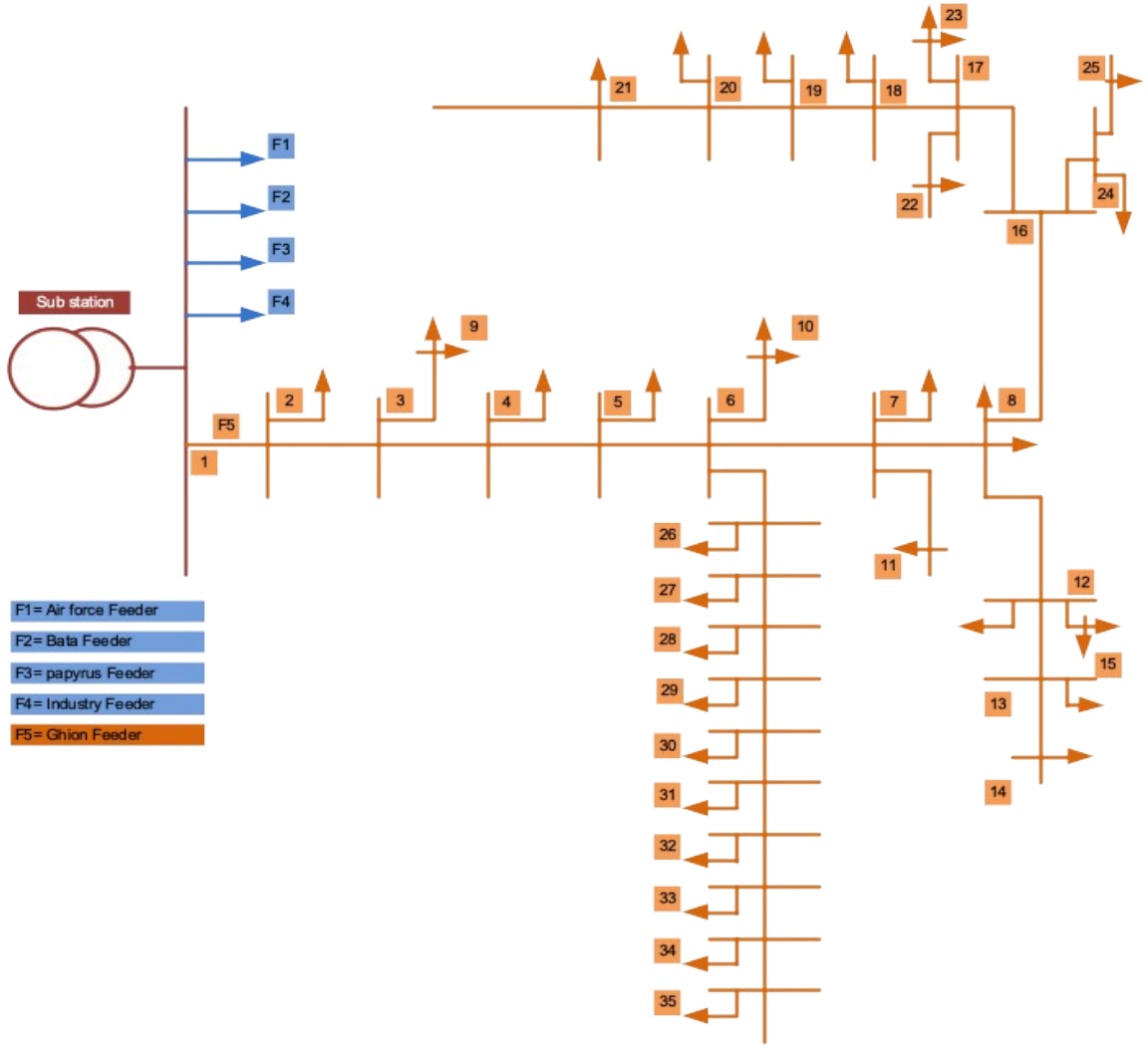

Figure 1: 35 Bus Ghion feeder of Bahir Dar distribution system

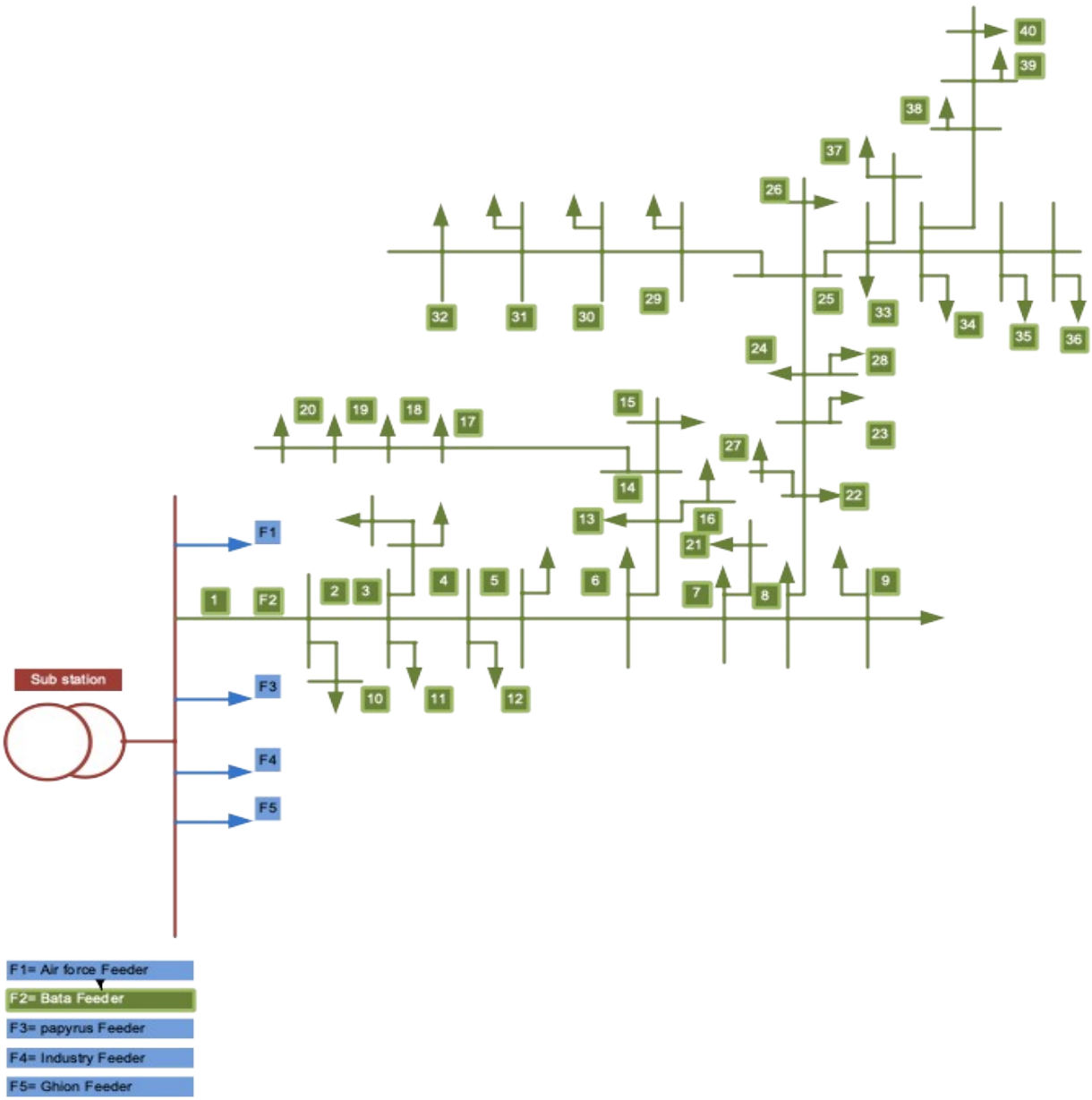

Figure 2: 40 Bus Bata feeder of Bahir Dar distribution system

3. Selection and Assessment of the Active and Reactive Power Generation Resources

This section discussed the selection and assessment of the distributed generation and reactive power supply sources utilized in this work.

3.1 Solar Photovoltaic (SPV) System

This work utilized the SPV system to generate the active power as distributed generation source [18] [19].

3.1.1 Power output of PV array

The out power of PV array is presented as,

$$P_{pv} = A_C \eta_{MP} \eta_E G_T \quad (1)$$

where, P_{pv} represents the output of PV array, A_C is the array area, $\eta_{mp}$is the maximum power point efficiency of the array (≈14%), η_e is the efficiency of power conditioning equipment (≈ 90%), and G_T is the incident solar radiation on the array.

3.1.2 Solar Radiation Estimations

Solar declination angle (δ) is the angle between the earth's equatorial plane and the earth sun line. Solar hour angle $\omega$is the angle Earth has rotated since solar noon. The relation between these angles is given by:

$$\delta = 23.45 \sin\left(360 \frac{284 + n_d}{365} ¿\right) ¿ \quad (2)$$

where, δ represents solar declinations angle (°), n_d is day number of the year starting at January 1^{st} as 1, ω is ($t_s - 12\,hr$ ¿.$15^{\circ}/h_r$, t_s is the solar time in hour, ω is solar hour angle (°). The value of $t_s$is 12 hrs at solar noon and 13.5 hours ninety minutes later.

$$\sin(\alpha) = \sin(\phi)\sin(\delta) + \cos(\phi)\cos(\delta)\cos(\omega) \quad (3)$$

where, α_s represents solar altitude (°) and ϕ is latitude (°).

$$\sin(\gamma_s) = \left[\frac{\cos(\delta)\sin(\omega)}{\cos(\alpha_s)}\right] \quad (4)$$

where, γ_s represents solar azimuz (°). The sunset/sunrise angle is given by

$$\omega_s = \cos^{-1}(-\tan\phi \tan\delta) \quad (5)$$

The solar angle of incident θ_i is the angle between the solar beam and normal to the solar panel, which is given by:

$$\cos(\theta_i) = [\sin\delta \sin\phi \cos\beta - \sin\delta \cos\phi \sin\beta \cos\gamma + \cos\delta \cos\phi \cos\beta \cos\omega + \sin\phi \sin\beta \cos\gamma \cos\omega + \cos\delta \sin\beta \sin\gamma si \quad (6)$$

The solar constant $(G ¿¿ sc)¿$ is equals to1367 W/m^2. The extraterrestrial irradiance on a surface at normal incidence (G_{on}) may be expressed as:

$$G_{on} = G_{sc}\left[1 + 0.033 \cos\frac{2\pi n_d}{365}\right] \quad (7)$$

The extraterrestrial irradiance incident on a horizontal plane at an arbitrary angle of incidence is expressed as:

$$G_o = G_{on}\cos(\theta_z) \quad (8)$$

where, θ_z is zenith angle between the solar beam and the vertical. $\theta_z$and $\theta$are not usually in the same plane. Integrating the solar constant (extraterrestrial irradiance) over the day length gives us the daily solar radiation on the horizontal surface.

$$H_o = \left(\frac{24 \times 3600}{\pi}\right) G_{sc} ¿ \quad (9)$$

where, δ is declination angle (°),and $\omega_s$is sunset hour angle (°). For Bahir Dar city the computed solar irradiance is as follows:

$Ho = 1367 * ¿$ =1,322.73W/m^2

3.1.4 Solar Energy Resource in Bahir Dar

Bahir Dar is located near the equator; its solar resource is obviously of significant potential. The annual average daily radiation in Bahir Dar reaching the ground is estimated to be 6kWh/m^2/day, which varies from a minimum of 5.26kWh/m^2/day in July to a maximum value of 6.86kWh/m^2/day in February [20]. Indirect estimation of solar radiation is performed by ground level measurement. Table 1 presented the estimated monthly solar radiation for Bahir Dar district.

Table 1: Estimated Monthly solar Radiation for Bahir Dar District (Lat = 11.4)

Mid of Month	N_d	$\delta(°)$	ω_s(°)	N(hours)	n	n/N	Ho(kW/m^2/d)	NMSA (kW/m^2/d)	NASA kWh/m^2/d	SWERAREL kWh/m^2/d

Jan	15	-21.270	87.326	11.644	9.78	0.84	9.25	6.40	6.27	6.335
Feb	45	-13.620	88.336	11.778	9.85	0.836	9.85	6.79	6.86	6.885
Mar	74	-2.819	89.662	11.955	9.56	0.8	10.36	6.98	6.78	7.072
Apr	105	9.415	91.138	12.152	8.91	0.733	10.47	6.76	6.01	6.491
May	135	18.792	92.337	12.312	7.23	0.587	10.22	5.95	5.78	6.089
Jun	166	23.314	92.960	12.395	6.83	0.551	9.22	5.66	5.35	5.867
Jul	196	21.517	92.708	12.361	5.87	0.475	9.98	5.36	5.26	5.392
Aug	227	13.784	91.685	12.225	6.79	0.555	10.04	5.85	5.91	6.122
Sep	258	2.217	90.266	12.035	8.35	0.694	10.29	6.50	6.29	6.68
Oct	288	-9.599	88.839	11.845	7.83	0.661	10.34	6.13	5.39	6.108
Nov	319	-19.148	87.616	11.682	8.57	0.734	9.98	6.05	5.69	6.258
Dec	349	-23.335	87.037	11.605	9.56	0.824	9.38	6.18	6.01	6.138
Avg	181.4	-0.752	89.99				9.04	6.218	5.96	6.286

For the renewable hybrid power system design of Bahir Dar, the estimated monthly average global solar radiation from the ground measured sunshine hour data from NMSA summarized and listed in table and utilized for the feasibility study of the proposed hybrid renewable energy system using HOMER.

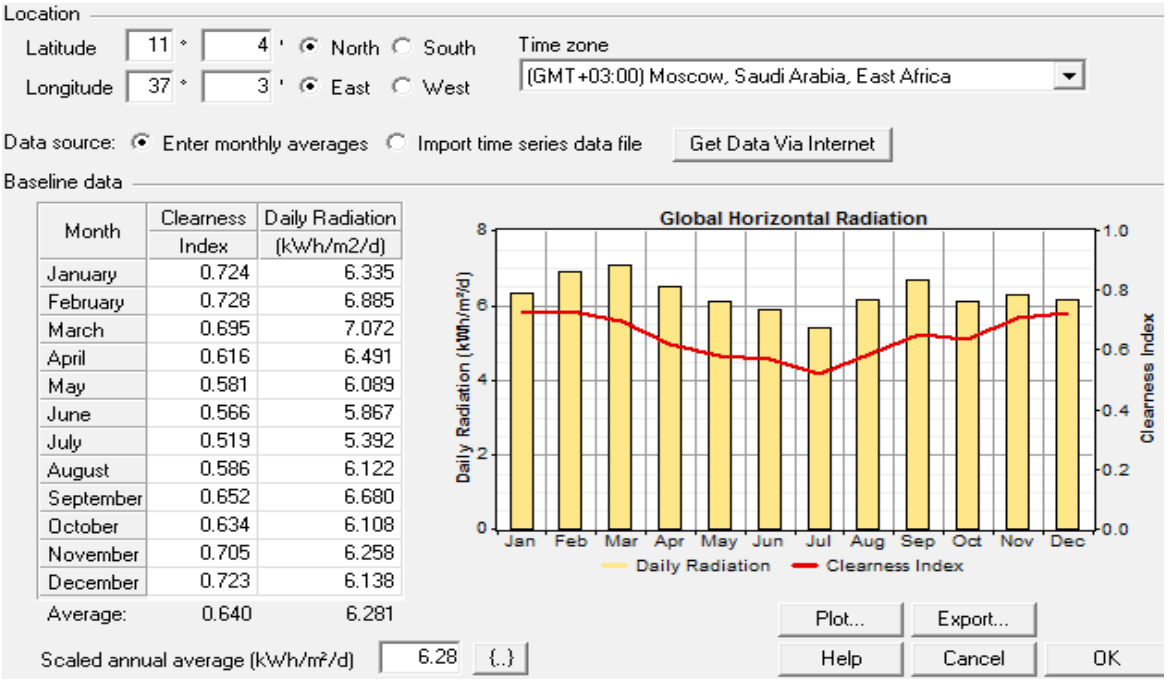

Figure 3: Monthly average solar radiation

Figure 3 presents the monthly average solar radiation calculated for Bahir Dar city by utilizing HOMER software.

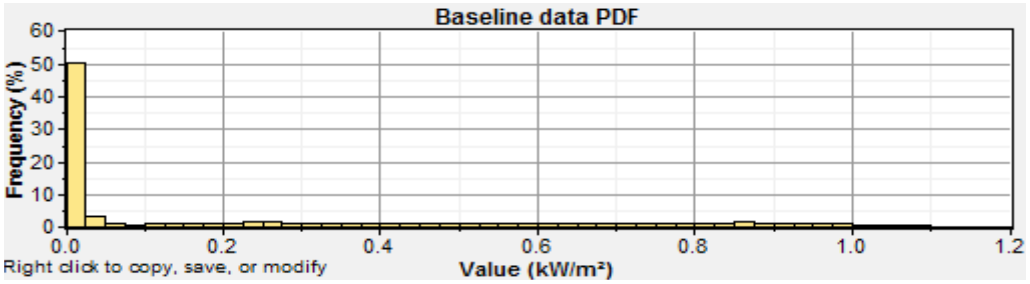

Figure 4: The solar power probability distribution

Figure 4 shows the solar power energy probability distribution calculated using HOMER software.

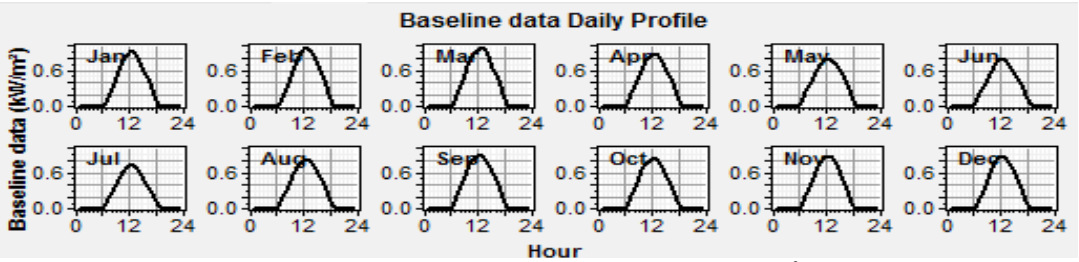

Figure 4: The daily sunlight radiation in kWh/m^2

3.2 Wind Turbine

The second distributed energy source utilized in this work is wind turbine.

3.2.1 Speed and Power Relations

The kinetic energy of wind in joules is presented by [18]:

$$Kinetic\ Energy = \frac{1}{2} m V^2 \tag{10}$$

where, m represents mass, V is wind speed.

The power generated in watts is given by [18]:

$$Power = \frac{1}{2} (Mass\ Flow\ per\ Second) V^2 \tag{11}$$

where, P represents mechanical power in the moving air (watts), ρ is air density (kg/m^3), A is area swept by the rotor blades (m^2), and V represents velocity of the air (m/sec).

The mechanical power output from the upstream wind is presented by,

$$P = \frac{1}{2} (\rho AV) V^2 = \frac{1}{2} \rho A V^3 \tag{12}$$

where, AV represents volumetric flow rate, and ρAV represents the mass flow rate of the air in kilograms per second. Power density of the selected area is used to compare two potential wind sites in watts per square meter and presented by:

$$Specific\ Power\ of\ Site = \frac{1}{2} \rho V^3 \tag{13}$$

3.2.2 Wind Speed Distribution

The mean wind velocity is given by,

$$V_{av} = \int_0^\infty v f(v)\, dv \tag{14}$$

The variation in wind speed is the best described by Weibull probability distribution function f with two parameters, the shape parameter k, and the scale parameter c. The following equation gives the probability of wind speed being v during any time interval:

$$f(u) = \left(\frac{k}{c}\right)\left(\frac{u}{c}\right)^{(k-1)} e^{-\left(\frac{u}{c}\right)^k} for\ 0<u<\infty, k>1, c>0 \tag{15}$$

The cumulative distribution $F(u)$ is given by,

$$F(u) = 1 - e^{\left(\frac{u}{c}\right)^k} \tag{16}$$

where, u is the wind speed, $k\,(¿0)$ is the shape parameter, and $c\,(¿0)$ is the scale parameter of the distribution. The value of the shape factor is varying from 1 to 4.

$$V_{ave} = \Gamma\left(1 + \frac{1}{k}\right) \tag{17}$$

$$\Gamma(x)=\int_0^{\infty}\xi^{x-1}\exp(-\xi)d\xi \wedge \Gamma(x)=\Gamma(x+1)=x\Gamma(x) \tag{18}$$

For *k=2;*

$$C=\frac{2}{\sqrt{\pi}}V_{ave} \tag{19}$$

Average wind speed and scale factor in equation are used to find the probability distribution using HOMER software. Figure 5 presents the wind probability distribution of the Bahir Dar city.

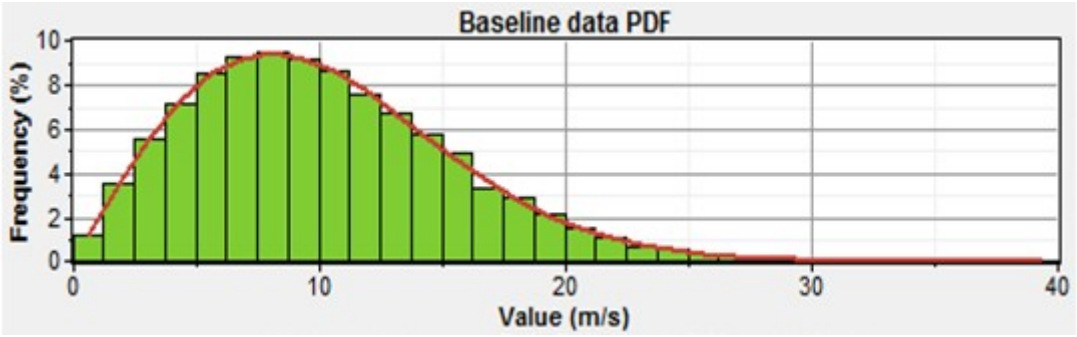

Figure 5: Wind probability distribution

The annual average wind speed for that hour is represented by the each of the 24 values of the average diurnal profile [18].

$$v_i=\bar{v}\left\{1+\delta\cos\left[\left(\frac{2\pi}{24}\right)(i-\phi)\right]\right\} \tag{20}$$

Daily wind profile obtained at height of 78 m of mean wind Speed of Bahir Dar is presented by the figure 6.

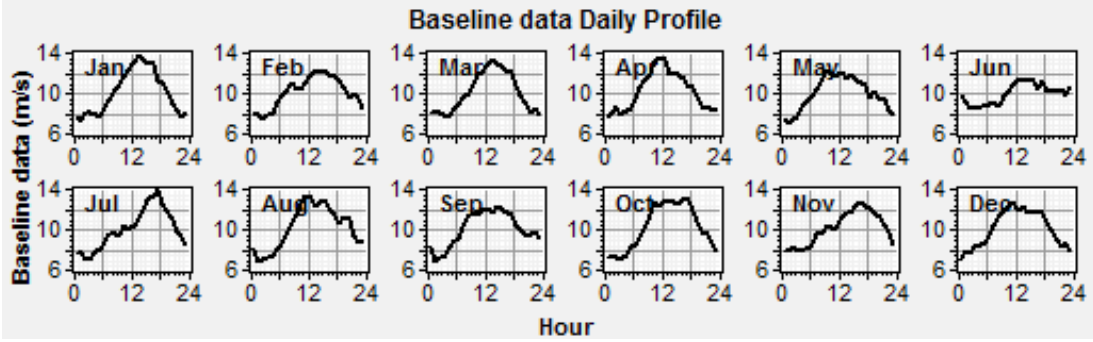

Figure 6: Daily wind profile in m/s of Bahir Dar city

3.2.3 Wind Power Density Distributions and Mean Power Density

The average power density is given by [18]:

$$P_{wm}=\frac{1}{2}\rho C^3\Gamma\left(1+\frac{3}{k}\right) \tag{21}$$

$$V_{ave}=C\Gamma\left(1+\frac{1}{k}\right) \tag{22}$$

Γ is the gamma function and given as:

$$for\,k=2\wedge\Gamma\left(1+\frac{3}{2}\right)=\frac{\frac{3}{2}*\sqrt{\pi}}{2}=3\frac{\sqrt{\pi}}{4} \tag{23}$$

The air density varies with the altitude and therefore the formula that governs this is:

$$\rho=\rho_o e^{-\left(\frac{0.297H_m}{3048}\right)}\vee\rho=\rho_o-1.194*10^{-4}H_m \tag{24}$$

Finally, power density for each month is given by:

$$P_{wm}=\frac{1}{2}\rho C^3\frac{3\sqrt{\pi}}{4} \tag{25}$$

The wind power density values of each month for Bahir Dar city is calculated and listed in table 2 below, where ρ equals to 1.225kg/m^3.

Table 2: Monthly Wind Power Density

Month	Bahir Dar city with k=2 Monthly Avg. wind speeds(m/s)	Scale factor	Power density(W/m^2) [Elev.=78m]
Jan	10.1	11.4519	1222.9
Feb	10.1	11.3535	1191.6
Mar	10.1	11.3706	1197
Apr	10.2	11.4745	1230.1
May	10.0	11.3070	1177
Jun	10.0	11.2623	1163.1
Jul	10.0	11.3396	1187.2
Aug	10.2	11.4853	1233.6
Sep	10.1	11.3492	1190.2
Oct	10.2	11.4870	1234.1
Nov	10.1	11.4345	1217.3
Dec	10.1	11.3606	1193.8
Monthly annual Avg.	10.1	11.3897	1203

The energy density characteristics at the height of 50 meter are presented in table 3 below.

Table 3: Wind energy output category benchmark [18]

Wind resource category	Wind level	Wind power density (W/m^2)	Wind speed at 50m (m/s)
Poor	1	50-200	3.5-5.6
Marginal	2	200-300	5.6-6.4
Moderate	3	300-400	6.4-7.0
Good	4	400-500	7.0-7.5
Excellent	5	500-600	7.5-8
Excellent	6	600-800	8-8.8
Excellent	7	Above 800	Above 8.8
Total area covered by marginal to excellent wind regions			

Observing the table 3, the power density category of Bahir Dar city is on the seventh category, which indicates the region, has very great potential for grid connected electric power generation. The technical data of Vestas V82 wind turbine as per the manufacturers data sheet is presented in table 4.

Table 4: Technical Data for Vestas V82 Wind Turbine Manufacturers' data sheet

Specification for VESTAS V82 Wind Turbine	
Available towers	59/70/78
Rotor	82 m diameter, 5.281m^2 swept area, 14.4 rpm
Cut-in wind speed	3.5 m/s
High wind speed	20 m/s
Rated power wind speed	1.65 MW at 13 m/s

Figure 7 presents a Vestas brand V82 model wind turbine power curve (which is used in this study) [19].

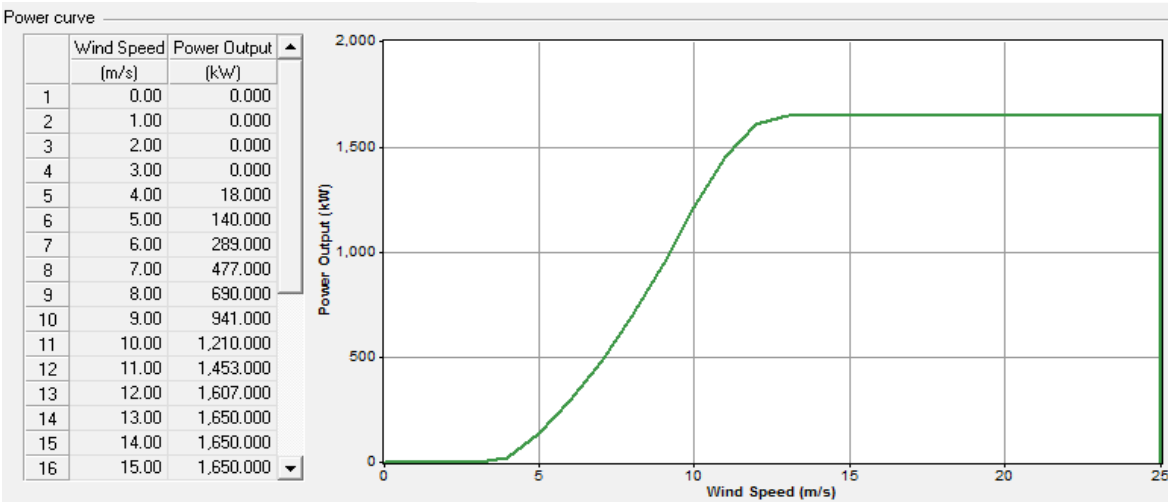

Figure 7: Power output curve with wind speed of Vestas V82 wind turbine

The output power of the WTG is varying between 0 to its power rating of 1.65 MW.

3.2.4 Wind Speed - Height Correction

The average wind speed increases with the height is approximately 1/7th of the power for the ideal smooth plane [18].

$$\frac{v(z_2)}{v(z_1)}=\left(\frac{z_2}{z_1}\right)^{\alpha} \tag{26}$$

where, $V(z_2)$ is the wind speed at the desired height of z_2; $v(z_1)$ is the wind speed measured at a known height z_1, and α is a coefficient known as the wind shear exponent. A modified formula is best suited for the estimation of the wind speed at hub height.

$$\frac{v(z_{hub})}{v(z_{anem})}=\frac{\ln\left(\frac{z_{hub}}{z_o}\right)}{\ln\left(\frac{z_{anem}}{z_o}\right)} \tag{27}$$

3.2.5 Wind Power Generation

As power generated for wind turbine is given by,

$$P=\frac{1}{2}\rho AV^3 \tag{28}$$

The air density ratio is provided by,

$$\frac{\rho}{\rho_o}=\left(1-\frac{BZ}{T_o}\right)^{g/RB}\left(\frac{T_o}{T_o-BZ}\right) \tag{29}$$

The air density under standard conditions i.e. at sea level and 15 degrees Celsius is 1.22kg/m^3. The hourly generation from wind turbine is given by,

$$\begin{cases} P_e=0\,(u<u_c) \\ P_e=a+bu^k\,(u_c\le u\le u_R) \\ P_e=P_{eR}\,(u_R\le u\le u_f) \\ P_e=0\,(u>u_f) \end{cases} \tag{30}$$

The coefficient *a* and *b* is given by:

$$a=\frac{P_{eR}u_{eR}{}^k}{u_c{}^k-u_R{}^k}\wedge b=\frac{P_{eR}}{u_R{}^k-u_c{}^k}$$

3.2.6 Annual Wind Energy Production and Capacity Factor

The capacity factor of wind turbine is given as [24]:

$$C_F = \left\{ \frac{\exp^{\left[-\left(\frac{u_c}{c}\right)^k\right]} - \exp^{\left[-\left(\frac{u_R}{c}\right)^k\right]}}{\left(\frac{u_R}{c}\right)^k - \left(\frac{u_c}{c}\right)} - \exp^{\left[-\left(\frac{u_F}{c}\right)^k\right]} \right\} \tag{31}$$

By utilizing $U_c = 3\,m/s, U_R = 13\,m/s, U_F = 20\,m/s, \wedge C = 10.43\,m/s$, the computed value of the capacity factor is 0.466. Therefore, the annual energy production of a single wind turbine is 6602587.2kWh by taking nominal rated power as 1650kW [18].

The minimum output power from cut in speed (i.e. 3m/s) is 26.27 kW power. The estimated capacity factor and annual energy production from a single Vestas V82 wind turbine are summarized in Table 5.

Table 5: V82 wind turbine estimated capacity factor and annual energy production [18]

District	Scale factor(C)	V_{av}	K	CF(capacity factor)	E(GWh)
BDR	11.3897	10.1	2	0.47	6.602587

The estimated capacity factor indicates that all values and annual energy production are within the acceptable range from a single Vestas V82 wind turbine.

3.3 Biomass Energy

The third distributed energy source utilized in this work is biomass energy source as it is widely available in Bahir Dar, Ethiopia. Bahir Dar is located in the north west of Ethiopia, where most of the country's agricultural crops are cultivated. Apart from huge availability of maize, beans, teff, barley and wheat in Gojjam and Gonder cities, which are near to Bahir Dar, the forest around the city, municipal solid waste (MSW), bio solids, industrial waste, animal manures, forestry residual, landscaping and tree clipping can be used as biomass resources. Figure 8 presented the Crop residue biomass resource in Gojjam, Bahir Dar, Ethiopia.

Figure 8: Crop residue biomass resource in Gojjam

Table 6 presented the Crop cultivation areas in the parts of Amhara region, near Bahir Dar, Ethiopia.

Table 6: Crop cultivation areas in some parts of Amhara region near Bahir Dar [21, 22]

District	Total area (hac)
Yilmama Densa	99,180
Quarit	61,473
Gozamin	121,807
Sinan	38,640
Farta	107,077
Lai-gaint	154,866
Banja	45,618
Guagusa-shikudad	30,432
Awi-zone	271,000
Sum	930,093

3.3.1 Physical Properties of Biomass

The content of moisture is estimated on the basis of dry and wet [21, 22]. On the wet basis moisture content is calculated as follows:

$$MC_W = \frac{mass\ of\ water}{mass\ of\ wet\ biomass} = h_{wet} = \frac{m_{tot} - m_{dry}}{m_{tot}} \times 100\,\% \tag{32}$$

Further, the estimation of the moisture content on the dry basis is calculated as,

$$MC_D = \frac{mass\ of\ water}{mass\ of\ dry\ wood} = h_{dry} = \frac{m_{tot} - m_{dry}}{m_{dry}} \times 100\,\% \tag{33}$$

where, m_{tot} represents the total mass, including moisture, m_{dry} represents the mass of the dry substance, and $m_{tot} - m_{dry}$ represents the moisture mass.

3.3.2 Heat Balance in a Complete Combustion

Generally the heat generated from the combustion is equals to the heat required for vaporizing the available water plus heat related to vaporize water mass and heat lost in the atmosphere. Higher heating value (HHV) and lower heating value (LHV) are the parameters utilized to calculate the amount of hear from the biomass. HHV represents the heat required for the combustion of per unit mass, while LHV is the subtraction of heat related to the vaporization of the existing water and water product from the heat required for combustion. The LHV for dry biomass is represented by,

$$LHV_{dry} = HHV_{dry} - 9\,Hq \tag{34}$$

where, *H* represents hydrogen content in dry biomass, which is 5 to7 % and q is water condensation heat, equals to 2.4 MJ/kg. The variation between HHV and LHV is normally equal to 1 to 1.5 MJ/kg. Actual amount of LHV calculated from LHV_{dry} is as follows:

$$LHV = (1-h)\,LHV_{dry} - hq = LHV_{dry} - h\left(LHV_{dry} - h\left(LHV_{dry} + q\right)\right) \tag{35}$$

where, h is moisture content on the wet basis.

In each ton of grain generally the ratio of dry matter at anthesis and final grin is among 1.29-1.50 t/ha. By taking an average of 1.4 ton/hectare, the total amount of biomass available is 1,302,130.2 tons. Table 7 presented the standard biomass moisture contents.

Table 7: Standard Biomass Moisture Contents [22]

Matter	Mwb	Mdb
Bagasse	50%	100%
Barley Straw	16%	19%
Corn Stover	30%	42%
Rice Straw	67%	200%
Wheat Straw	12%	14%
Forest Residues	44%	78%
Primary Mill Residues	48%	91%
Urban Wood Residues	10%	14%

The efficiency and capacity of power plant decrease as co firing ratio of biomass increases

$$Efficiency\ Drop = -0.4\,(co-fire\ ratio)^2 + 0.12\,(co-fire\ ratio)$$

$$P_e = P_{e.org} = \frac{\eta_{Biomass}}{\eta_{org}} \tag{36}$$

For calculating the biomass and coal needed in co-firing system is calculated as,

$$\frac{t.biomass}{year} = Power\ Plant\ ¿\ Co-fire * Capacity\ Factor * 8760\frac{hrs}{yr} * Heat\ Rate * [HHV]_{biomass}^{-1} \tag{37}$$

In this work, the capacity factor is selected as 80%. For normal operating conditions, the total biomass required by the power plant to generate 2.7 MW with co-firing capacity of 5%, heat rate 80% and HHV 80% is as follows:

$$\frac{t.biomass}{year} = 2700 * 0.05 * 0.8 * 8760 \frac{\frac{hrs}{yr} * 1}{0.8} = 1182600\, tons/year$$

3.4 Shunt Capacitor Modelling

For supply the reactive power support, shunt capacitor (QGs) are utilized. The advantages of shunt capacitors are lower cost, improved voltage profile, and reduced losses. The maximum amount of capacitance value required can be calculated as follows [11]:

$$Q_{max} = U \times Q_o \tag{38}$$

where, U is an integer. In this work U is taken as 9. Therefore, the required value of QG is 1.35 MVAr.

4. Methodology and Problem Formulation

This section discusses the problem formulation for the optimal placement and sizing of the DGs and QGs resources utilized in this work by using multi objective whale optimization algorithm (MWOA).

4.1 Optimal placement and Sizing of DGs and QGs for the Radial distribution network Using MWOA

The backward/forward load flow is used for performing the load flow analysis of the selected distribution network. In the process of optimization, active and reactive powers are injected from DG and QG, respectively based on the feeder current carrying capacity. It is less than the peak load i.e. sum of the power loss and power demand. In this work, to make the integration and compensation safe from the reverse current flow, it is taken as 80% of the limit as a network optimization constraint. While performing the system optimization for the radial distribution network using load flow, one should satisfy all the constraint conditions to meet the objective of the proposed problem. The ultimate goal of this work is to minimize the aggregate active power loss in the distribution network. This can be given as:

$$min\, P_{loss} = \sum_{i}^{N} I_i^2 R_i \tag{39}$$

where, I_i, $R_i$and N are the current, resistance and number of buses, respectively.

To optimize the above objective function under constraint conditions, the power flow equation should satisfy all the equality constraints presented below:

$$P_{¿} + P_{DG} = P_{loss} + P_{load} \tag{40}$$

$$Q_{¿} + Q_{shunt} = Q_{loss} + Q_{load} \tag{41}$$

where $P_{¿}$ and $Q_{¿}$are the aggregate active and reactive power, injected by the sub-station into the network, P_{DG} and Q_{shunt} are the gross real and reactive power, injected by the DG and QG, respectively. $P_{loss}$and Q_{loss} are the aggregate active and reactive power losses in the network. $P_{load}$and Q_{load} are the gross active and reactive demands of the system.

The inequality constraints are as follows:

Voltage constraints are given by:

$$V_{min} \le V_i \le V_{max} \tag{42}$$

where, V_{min} is set to 0.95 and V_{max} is fixed to 1.05.

Feeder integrating capacity [15, 16] is limited by its maximum thermal loading limit i.e.

$$I_{li} \le I_{li,rated} \tag{43}$$

Location of DG (under the assumption that first bus is taken as slack bus)

$$2 \le DG_{position} \le n_{buses} \tag{44}$$

4.2 Whale Optimization Algorithm (WOA)

WOA is the recent meta-heuristic algorithm developed by Mirjalili and Lewis [17] in the year of 2016. The whales are highly intelligent animals. WOA is inspired by the special hunting behavior of the humpback whales, which prefer to hunt krill or small fishes, closer to the surface of sea. Humpback whales special hunting called

bubble net feeding method. For hunting, they swim around the prey and create distinctive bubbles along a circle or 9-shaped path [17].

From the basic characteristic of hunting, the following points are observed from the WOA.

4.2.1 Encircling prey

One character of Whales predicts the current position is exact and in circles the prey. This character of social behavior is transformed in the mathematical equation, as the current best candidate solution set in the objective function. All other social groups will try to update their position status towards the best hunter. The behavior modeled is as:

$$\overrightarrow{X(t+1)} = \overrightarrow{X^{¿}(t)} - \vec{A}.\vec{D} \tag{45}$$

$$\vec{D} = \left|\vec{C}.\overrightarrow{X^{¿}}(t) - \vec{X}(t)\right| \tag{46}$$

$$\vec{A} = 2.\vec{a}.\vec{r} - \vec{a} \tag{47}$$

$$\vec{C} = 2.\vec{r} \tag{48}$$

where, $\overrightarrow{X^{¿}}, \vec{X}$ represent current position of best solution and position vector. Current iteration is denoted by t. $\vec{A}, \vec{C}$ are coefficient vectors. $\vec{a}$ is directly decreased from 2 to 0. $\vec{r}$ is random vector [0,1].

4.2.2 Bubble net hunting method

In this hunting, character of whales, used two methods,

1. This time the whale encircles the prey and then shrinks from the far to the centre: Here $\vec{A} \in [-a, a]$ where $\vec{A}$ is decreased from 2 to 0. Position $\vec{A}$ is setting down at random values in between [-1, 1]. The new position $\vec{A}$ is computed in between previous position and position of the current best agent.

2. Spiral position updating: The whale shows a mimic helix-shaped movement to the prey, this property of whale can be represented in spiral equation:

$$\vec{X}(t+1) = \overrightarrow{D'}.e^{bl}.\cos(2\pi l) + \overrightarrow{X^{¿}} \tag{49}$$

Prey may use more than two paths simultaneously, when whales hunt. In this work, 50% probability (*Prob*) is taken for the above two methods.

$$\vec{X}(t+1) = \begin{cases} \overrightarrow{X^{¿}}(t) - \vec{A}.\vec{D}, \wedge if\ Prob < 0.5 \\ \overrightarrow{D'}.e^{bl}.\cos(2\pi l) + \overrightarrow{X^{¿}}, \wedge if\ Prob \geq 0.5 \end{cases} \tag{50}$$

where, $D' = \left|\overrightarrow{X^{¿}} - \vec{X}(t)\right|$ the distance between whale and the prey. b is the constant, $l \in [-1,1]$. *Prob* is the arbitrary number from [0, 1]. Equation (49) presents the spiral updating position.

3. To get the global possible optimum, updating has done with randomly

$$\vec{D} = \left|\vec{C}.\overrightarrow{X_{rand}} - \vec{X}\right| \tag{51}$$

$$\vec{X}(t+1) = \overrightarrow{X_{rand}} - \vec{A}.\vec{D} \tag{52}$$

$\overrightarrow{X_{rand}}$ is the random whale in current iteration.

4.3 Implementation of MWOA

Here the MWOA is implemented using program algorithm with and without bound called by same iteration and fitness limit. This is presented in figure 9 and performed as follows:

1. On the first sequence phase, he whales will be initialized first then passed within the limits of DG/QG and the number of iterations.
2. On the second sequence, it will check with the same program beyond the limits of DG/QG to search the new fitness boundary.
3. Lastly, the value of optimization which is the most minimum loss will be recorded.

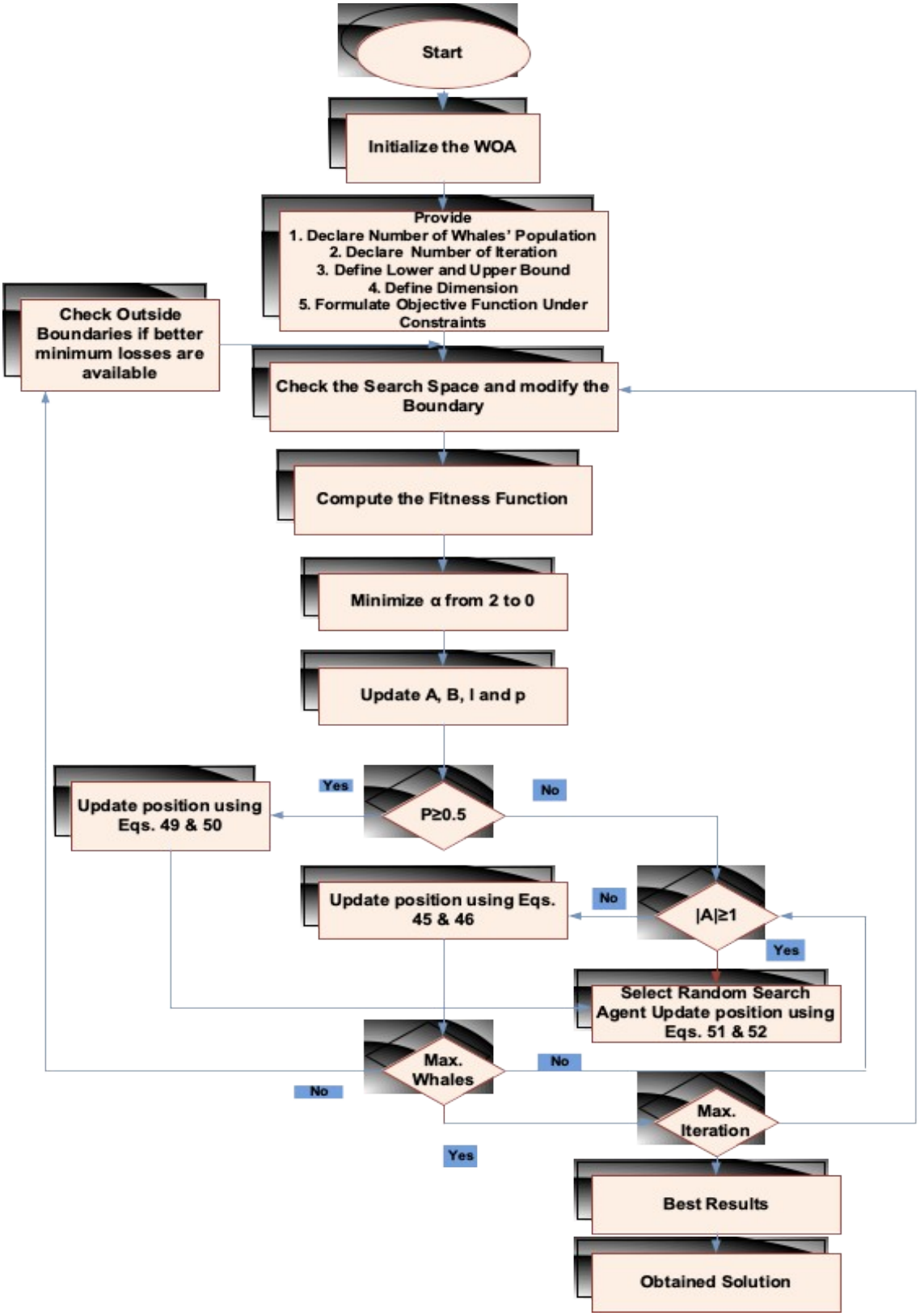

Figure 9: Flow Chart of MWOA algorithm

The algorithm utilized in this work is as follows [17]:

Step 1: Read 80% of the peak load of the feeder

Step 2: Initialize the population

Step 3: Generate the population of DG/QG sizes randomly using equation population = $(DG/QG_{max} - DG/QG_{min}) \times rand() + DG/QG_{min,}$ where DG/QG_{min} and DG/QG_{max} are the minimum and maximum limits of DG/QG sizes.

Step 4: Solve the feeder-line flow

Step 5: Find power losses for the generated population.
Step 6: If there is possible minimum power loss, search out of DG/QG limit, consider only the network limit.
Step 7: Set similar program out and call it to step 3.
Step 8: Current best solution DG and QG values with low losses.
Step 9: For updated population repeat step 6 and 7
Step 10: If obtained losses are less, then replace current best solution with it or else go back to step 7.
Step 11: Record results if tolerance is <0.001 or go to step 2
Step 12: By using Equations. (45) – (52) update the position of whales.

5. Numerical System Study and Comparative Analysis

Real power loss minimization by using integrating active and reactive power source is applied to the two critical feeders of Bahir Dar radial distribution network. These feeders are connected from the Bahir Dar substation-II 400/230/66/15 kV bus. Feeder 5 is named as Ghion, which has 35 buses while the other feeder named as Bata feeder has 40 buses.

Using the line and load data of the selected radial distribution network, backward/forward sweep load flow is performed to get the total feeder loss and initial voltage profile of the selected buses. In reasonable condition, without any optimization, the total active load at the Bata feeder is 1.8262 MW with 1.5353 MVAr reactive loads. Ghion feeder has 3.43257 MW active and 2.5776 MVAr reactive loads. In addition to this, the initial loss at the Bata feeder is 0.1262149 MW, and Ghion feeder is 0.3395703 MW.

In this work, for the system loss minimization, DG and QG sources are optimally sized and placed at the selected feeders by MWOA optimization method. MWOA results are compared with the multi-objective MPSO. The method is implemented using a MATLAB R2016 programming language with computer properties of 2.2 GHz processer and 7.58 GB RAM with core i7. The MATLAB program code is executed using the WOA algorithm. The proposed method aimed to minimize real power loss by optimizing the objective function under constraint conditions. For comparison purpose, the parameters of the controlling values of MPSO are set as: the number of iterations is equal to 100, w is equal to 0.95, C_1 is equal to 2, C_2 is equal 2. In the case of MWOA, the iteration is the same as MPSO and the dimensions (dm) representing the total active power is set to one. The first bus is selected as the slack bus. The results are discussed in the following sub-sections.

5.1 Ghion Feeder Optimization

5.1.1 Real Power Loss Minimization

The result of the load flow provides the total real line losses as 339.5703 kW. When DG and QG are used as the source of optimization in the Ghion feeder, as seen from table 8, the feeder total active power loss after MWOA optimization is reduced to 22 kW. For the comparative analysis, by implementing the MPSO optimization, the loss reduced to 27 kW. From the above result, it is clear that the total power saved after the implementation of MWOA is 317.6 kW while with MPSO is 312.6 kW for Ghion feeder. Therefore, results concluded that MWOA provided better results as compared to MPSO. Figure 10 presented the comparative analysis of power losses of Ghion feeder before and after the optimization performed by MWOA and MPSO.

Table 8. Result summary of Ghion feeder buses

Method	P_{loss} (kW)	DG size	QG size	Location DG	Location QG	V_{avg}
Load flow	339.5703	-	-	-	-	0.96
MPSO	27	3.16	1.709	28	27	0.988
MWOA	22	1.822	0.280	16	17	0.99

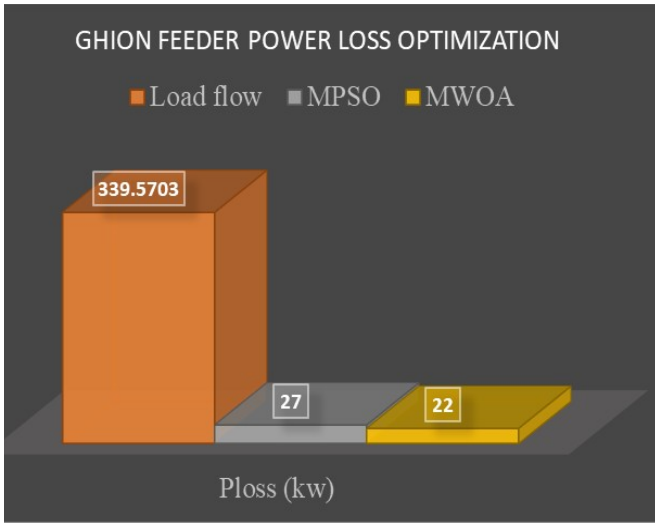

Figure 10: Power loss minimization in Ghion feeder before and after the optimization

5.1.2 Voltage Profile Improvement

After the placement of DG and QG, the voltage profile is also upgraded. The load flow indicates that the average voltage profile of the feeder before the optimization is about 0.961 p.u. The profile after the optimal sizing and placement of DG and QG by using MWOA is improved to 1.0258 p.u while with MPSO is improved to 0.988 p.u. The per branch profile of voltage after and before the optimization is shown in figure 11.

The minimum value of voltages, before the placement of DG and QG are 0.9436 p.u (at bus 35) and 0.9437 p.u (at bus 34). With the MWOA optimization of the system, which is used for the placement and size of DG and QG, the value of voltages at the mentioned buses are improved to 1.0189 p.u (at bus 35) and 1.0194 p.u (at bus 34), while with the MPSO optimization, the values of voltages are improved to 0.9955 p.u (at bus 35) and 0.9960 p.u (at bus 34).

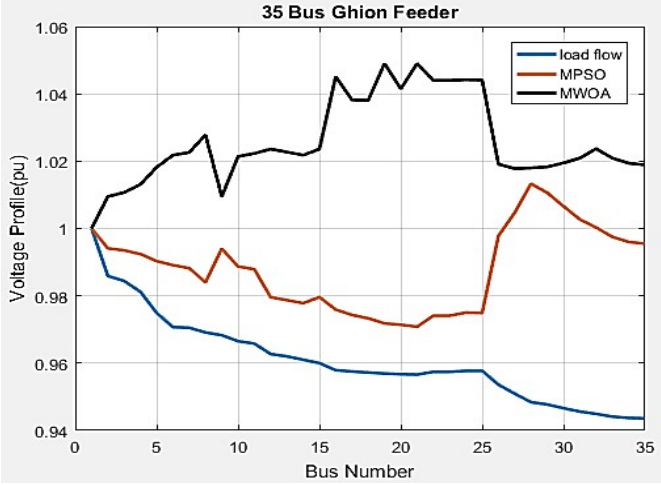

Figure 11: Voltage profile improvement of the 35-bus Ghion feeder before and after the optimization

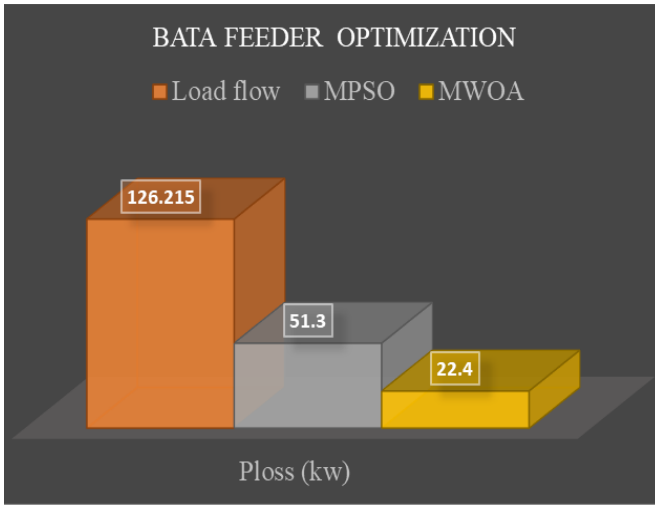

Figure 12: Power loss minimization in Bata feeder before and after the optimization

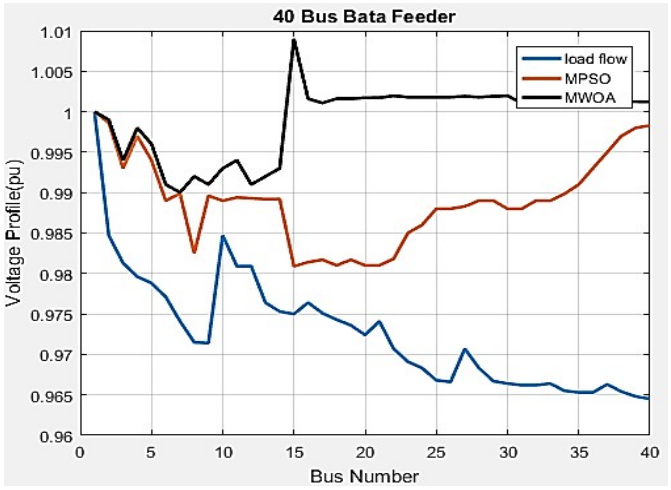

Figure 13: Voltage profile improvement of the 40-bus Bata feeder before and after the optimization

Figure 11 presented the comparative analysis of voltage profiles of Ghion feeder before and after the optimization performed with MWOA and MPSO.

5.2 Optimization of Bata Feeder

5.2.1 Real Power Loss Minimization

The result of the load flow provides the total real line losses as 126.2149 kW. In the optimization process of the 40-bus Bata feeder by optimally integrating DG and QG, as seen from the Table 9, the aggregated active power loss calculated by MWOA is reduced to 22.4 kW while with MPSO reduced to 51.3 kW. From the results, it is clear that total power saved after MWOA optimization is 103.814 kW while with MPSO is 74.914 kW. Figure 12 presented the comparative analysis of power losses of Bata feeder before and after the optimization performed with MWOA and MPSO.

Table 9. Result summary of Bata feeder buses

Method	P_{loss} (kW)	DG size	QG size	Location		V_{avg}
				DG	QG	
Load flow	126.215	-	-	-	-	0.9727
MPSO	51.3	1.437	1.1434	25	24	0.989
MWOA	22.4	0.820	1.070	35	31	0.999

5.2.2 Voltage Profile improvement of Bata Feeder

After the optimal placement of DG and QG, the voltage profile of various buses the Bata feeder is improved. The average voltage profile of the feeder before the optimization is 0.9727 p.u. The voltage profile after optimally placing the DG and QG with the help of MWOA is improved to 0.9991 p.u while with MPSO it is improved to

0.9890 p.u. Figure 13 presented the comparative analysis of voltage profiles of Bata feeder before and after the optimization, performed by MWOA and MPSO.

5.3 Performance Comparison Study of Existing System with MWOA and MPSO

This work optimizes the real power loss minimization problem by satisfying all the constraints. The active power loss is reduced, and the voltage profiles are improved. It is often robust to consider feeder voltage regulation related to the profiles of feeder voltage. Voltage profile indicates the magnitude of the voltage with respect to its location on the feeder. One way to determine the quality of power is maintaining the receiving end voltage magnitude closer the same to the sender end. For bring this achievement practically, the capacitor and distributed generation are applied in this work for Bahir Dar distribution system. The size and placement of distributed generation and shunt capacitor are performed by MWOA which illustrated using the thirty-five-bus Ghion feeder and forty-bus Bata feeder, the practical feeders of the Bhir Dar distribution system. The real power losses, DG and QG sizes with location and average voltage profile of these feeders before and after the optimization is presented in TABLE III and IV.

Optimal location and size of DG and QG are found with the help of MWOA and compared with MPSO. After optimization, the power loss had reduced from 339.5703 kW to 22 kW in Ghion feeder and from 126.2149 kW to 22.4 kW in Bata feeder using MWOA. It had reduced from 339.5703 kW to 27 kW in Ghion feeder and from 126.2149 kW to 51.3 kW in Bata feeder using MPSO.

The algorithm developed for the power loss reduction by applying shunt compensation of capacitor and DG integration had improved the overall system voltage profile. As a result, the voltage profile before the optimization is 0.96, after optimization with MPSO, it is improved to 0.988 pu, and after optimization with MWOA, it is improved to 0.997 p.u for Ghion feeder. The voltage profile of Bata feeder before and after optimization is 0.9726. After optimization with the MPSO is improved to 0.989 and with MWOA improved to 0.9991 p.u in Bata feeder. From the results, it is clear that MWOA provided better performance as compare to the MPSO optimization approach.

5.4 Power Output from various sources

The wind power density and the capacity factor of Bahir Dar is very suitable for wind generation. Hence, two wind turbines are considered in this study to supply the main power demand. Rest demand which is not covered by the wind generation is supplied by solar power. The output of Vestas V82 wind turbine at average speed of 10.43 m/s is 1210 kW. Therefore, the total generation from two wind turbines is 2410 kW.

The required solar power is (2700kW -2410kW) 290 kW. The daily average solar radiation of Bahir Dar city is 6.286 kWh/m^2/d. The solar irradiance computed for the Bahir Dar city is 1,322.73W/m^2. The solar power output at 1322.73W/m^2 is about 190 W with this about 1527 solar panels are required.

Biomass resource is utilized as the backup source in this work. To minimize the investment cost of the biomass, it should be installed at 16th bus of Ghion feeder and 35th bus of Bata feeder. The total DG value calculated from WOA optimization is about 2.7 MW. Since biomass is utilized as back up, its value should equal to the total power demanded from DG i.e. 2.7 MW. For normal operating conditions, the total biomass required by the power plant to generate 2.7 MW with co-firing capacity of 5%, heat rate 80% and HHV 80% is 1182600 tons/year.

The QG value of the two feeder after WOA optimization is 1.35MVAr. The value of QG can be found in multiple of 150 KVAr.

5.5 Investment Cost of Overall System

For the development of wind, solar and biomass power plant based distributed generation system, the investment cost and shunt capacitor cost is summarized in table 10 [18], [23]:

Table 10: Expected cost of DG and QG in USD/W and kVAr

Technology	Investment cost($/W)	Capacitor cost($/kVAr)
Biomass	1.5-2.5	
Wind	0.8-1.5	5
Solar PV	6-8	

The investment cost of the system, optimized using WOA for the selected two feeders is presented in table 11. Since wind capacity factor is higher, it is reasonable to choose two wind turbines and the rest should be solar energy. The biomass is utilized as backup source to avoid intermittence nature of wind and solar energy. Hence, it would cover all the power supplied by solar and wind during their off condition. Further, shunt capacitor is utilized to supply the reactive power, required by the system.

Table 11: Total Investment Cost

Technology	Size	Investment cost($)
Biomass	2.7(MW)	4,050,000-10125000
Wind	2.41(MW)	1928000-2892000
Solar, PV	0.29(MW)	1740000-13920000
QG	1.35 (MVAr)	6750
Total investment cost		7724750-26943750
Average of total investment cost		17,334,250

6. Conclusion

Localizing the active generation and reactive power demands had reduced the power loss. In this research, multi-objective-based optimizations were applied in two ways for the search algorithm. In the first sequence whenever the natural search within the defined size of DG/QG is quite enough to get the minimum loss, the whales/Particles will just finish the search for optimization in the natural optimization techniques. In the second attempt, however, is if they get the better total minimum power loss outside of DG/QG boundary they (Whales/Particles) will go for search and adjust the searching space for the size of DG/QG and the power loss result.

As a result of this character, the voltage and power output might not be sharp like the natural optimization techniques since it is long-pressing search for total minimum active loss priority. Therefore, this technique of optimization has reduced the current flowing in each branch of the feeder. It is further reduced the loss of the line. Substantially, the voltage drop in the branch of each feeder is also reduced.

In this work, two practical feeders of the Bahir Dar distribution network was considered to perform the loss minimization as well as voltage profile improvement of the system. MWOA was compared with the MPSO, which shows the superiority of the initial one. As the future enhancement of this work, whole Bahir Dar distribution network can be considered under different constraints conditions of the power system for the better understanding of the system performance. Further, more objectives can be incorporated in the objective function, for further optimized the system.

Acknowledgement

This work was supported by VILLUM FONDEN under the VILLUM Investigator Grant (no. 25920): Center for Research on Microgrids (CROM); www.crom.et.aau.dk

Conflict of Interest

The authors declare no potential conflict of interest

References

[1] Tom Short, Trishia Swayne, "Assessment of Transmission and Distribution Losses in New York PID071178 (NYSERDA 15464)," The New York State Energy Research and Development Authority, New York, November 2012.

[2] Ola Badran, Saad Mekhilef, Hazlie Mokhlis, Wardiah Dahalan, Optimal reconfiguration of distribution system connected with distributed generations: A review of different methodologies, Renewable and Sustainable Energy Reviews, Vol. 73, 2017, PP. 854-867.

[3] Abid Ali, Nursyarizal Mohd Nor, Taib Ibrahim, Mohd Fakhizan Romlie, "Sizing and placement of battery-coupled distributed photovoltaic generations," Journal of Renewable and Sustainable Energy, vol. 9 issue 5, 2017.

[4] M. Padma Lalitha, P. Suresh Babu, B. Adivesh, "Optimal Distributed Generation and Capacitor Placement for Loss Minimization and Voltage Profile Improvement using Symbiotic Organisms Search Algorithm," International Journal of Electrical Engineering, vol. 9, no. 3, pp. 250-262, 2016

[5] A.Y. Abdelaziz, E.S. Ali, S.M. Abd Elazim, Optimal sizing and locations of capacitors in radial distribution systems via flower pollination optimization algorithm and power loss index, Engineering Science and Technology, an International Journal, Vol. 19, Issue 1, 2016, PP. 610-618.
[6] P. D. P. Reddy, V. C. V. Reddy, and T. G. Manohar, "Whale optimization algorithm for optimal sizing of renewable resources for loss reduction in distribution systems," Renewables Wind, Water, and Solar. pp. 1–13, 2017.
[7] Wang C. et al. (2011) Reactive Power Optimization Based on Particle Swarm Optimization Algorithm in 10kV Distribution Network. In: Tan Y., Shi Y., Chai Y., Wang G. (eds) Advances in Swarm Intelligence. ICSI 2011. Lecture Notes in Computer Science, vol 6728. Springer, Berlin, Heidelberg.
[8] Suman Bhullar and Smarajit Ghosh, "Optimal Integration of Multi Distributed Generation Sources in Radial Distribution Networks Using a Hybrid Algorithm," Energies, vol. 12, no. 4-5, pp. 2-15, 2018.
[9] Xie, Jun & Liang, Chunxiang & Xiao, Yichen. (2018). Reactive Power Optimization for Distribution Network Based on Distributed Random Gradient-Free Algorithm. Energies. 11. 534.
[10] Christeen G.Boktor, Abdel-Raheem Youssef, Asmaa H. Ali,Salah Kamel, "Optimal Distribution Power Flow Including Shunt Capacitor Allocation Based on Voltage Deviation and Power Loss minimization," in 2017 Nineteenth International Middle East Power Systems Conference (MEPCON), Menoufia University, 2017.
[11] Ahmed Elsheikh, Yahya Helmy, Yasmine Abouelseoud, Ahmed Elsherif, Optimal capacitor placement and sizing in radial electric power systems, Alexandria Engineering Journal, Vol. 53, Issue 4, 2014, PP. 809-816.
[12] V. V. Thang,N. D. Minh, "Optimal Allocation and Sizing of Capacitors for Distribution Systems Reinforcement Based on Minimum Life Cycle Cost and Considering Uncertainties," The Open Electrical & Electronic Engineering Journal, vol. 11, no.18, 2017 pp. 165-176
[13] Hamid HassanzadehFard, Alireza Jalilian, Optimal sizing and location of renewable energy based DG units in distribution systems considering load growth, International Journal of Electrical Power & Energy Systems, Vol. 101, 2018, PP. 356-370.
[14] D.B. Prakash, C. Lakshminarayana, Optimal siting of capacitors in radial distribution network using Whale Optimization Algorithm, Alexandria Engineering Journal, Vol. 56, Issue 4, 2017, PP. 499-509.
[15] Kumar, M.; Nallagownden, P.; Elamvazuthi, I. Optimal Placement and Sizing of Renewable Distributed Generations and Capacitor Banks into Radial Distribution Systems. Energies 2017, 10, 811.
[16] Mahesh Kumar, Perumal Nallagownden, Irraivan Elamvazuthi, "Multi-objective PSO based optimal placement of solar power DG in radial distribution system," J. Electrical Systems, vol. 13, no. 2, pp. 322-331, 2017.
[17] Seyedali Mirjalili, Andrew Lewis, The Whale Optimization Algorithm, Advances in Engineering Software, Vol. 95, 2016, PP. 51-67.
[18] M. R. Patel, Wind and Solar Power Systems Design, Analysis, and Operation, New York, U.S.A.: CRC Press, 2006.
[19] Priscila Gonçalves Vasconcelos Sampaio, Mario Orestes Aguirre González, Photovoltaic solar energy: Conceptual framework, Renewable and Sustainable Energy Reviews, Volume 74, 2017, Pages 590-601.
[20] "Solar Power System," Free Energy Planet, 12 January 2017. [Online]. Available: https://www.freeenergyplanet.biz/solar-power-systems/solar-photovoltaic-power-system-1.html. [Accessed on 28th May 2020].
[21] Yazie Chanie1 *, Akalu Teshome1 , Yalfal Temesgen1 and Baye Berihun. Characterization of potato production, marketing, and utilization in North Western Amhara Region, Ethiopia, Journal of Horticulture and Forestry, Vol. 9(3), pp. 17-25, March, 2017.
[22] Jennie Jorgenson, P. G. (2011, 09). Technical Manual for the SAM Biomass Power Generation Model. https:// www.nrel.gov/docs/fy11osti/52688.pdf. [Accessed on 23rd Aug., 2020].
[23] S. Soleymani, B. Mozafari, M. A. Kamarposhti. (2014). Optimal Capacitor Placement for Power Loss Reduction and Voltage Stability Enhancement in Distribution Systems. Trakia Journal of Sciences, 12, pp 425-430.